Research on temperature control of adiabatic demagnetization refrigerators

Peng Zhao[1,2], Ke Li[1*], Yanan Li[1,2], Xiaotao Wang[1], Wei Dai[1,2], Jun Shen[1,2*]

[1] State Key Laboratory of Cryogenic Science and Technology, Technical Institute of Physics and Chemistry, Chinese Academy of Sciences, Beijing 100190, China
[2] University of Chinese Academy of Sciences, Beijing 100049, China

[*]E-mail: vlike87@163.com (K. Li), jshen@mail.ipc.ac.cn (J. Shen)

Abstract. In astronomical observations, detectors operating in the sub-Kelvin temperature range require extremely stable working temperatures. Adiabatic demagnetization refrigerators (ADR), as the sub-Kelvin refrigerators that are independent of gravity and offer high temperature control precision, have become the preferred choice for astronomical observation missions. The high temperature control precision originates from the intrinsic nature of ADR, which generates cooling power through demagnetization. By controlling the demagnetization rate through PID control, high stability in the order of μK can be achieved. Here we present the study of temperature control for the second stage of a two-stage ADR. The influence of environmental noise has been analyzed. The effects of the PID control strategy, magnet power supply resolution, and temperature measurement filtering on temperature fluctuations have been investigated. In the presence of noise interference, the Root Mean Square Error (RMSE) of isothermal demagnetization at 49 mK over 1.6 hours is 4.12 μK. During the brief noise-source-off period, a 262 second interval exhibited an RMSE of 1.99 μK, demonstrating potential for further improvement in the system's temperature control performance.

1. Introduction

Sub-Kelvin temperatures are indispensable in certain astronomical observations[1,2], where sensors operating at these ultra-low temperatures achieve high resolution to detect extremely faint incoming signals[3]. To ensure detector precision, their operational temperature should be maintained within a stable range, thus necessitating strict control over thermal fluctuations that could compromise resolution performance[4–6].

Mainstream sub-Kelvin refrigerators include dilution refrigerators (DR), adsorption refrigerators (AR), and adiabatic demagnetization refrigerators (ADR)[7]. Among these, ADR have not only been used in ground-based applications but have become the important cooling solution for space-based observations due to their gravity-independent operation[8–11]. The entropy of magnetocaloric materials serving as ADR refrigerants is a function of temperature and magnetic field. Utilizing this property, precise temperature control is achieved by regulating magnetic field variations at appropriate rates. In the ADR, superconducting magnets generate controllable magnetic fields through current regulation, with the temperature controlled by the magnetic field, thereby ensuring the ability to achieve high temperature stability. We conduct temperature

control studies for isothermal demagnetization of ADR at 49 mK based on PID control. The study is organized as follows. Section 2 describes the experimental system, in which environmental noise interference on temperature measurements is investigated and enhanced shielding measures are implemented. Section 3 introduces the temperature control system and its control strategy. Section 4 investigates the temperature control performance under different PID outputs (current or voltage) and two types of magnet power supplies. Finally, Section 5 summarizes the research.

2. Experimental system and environment

2.1 Experimental system

The ADR system employs a GM-type pulse tube cryocooler for precooling, providing a ~4 K heat sink. As shown in Figure 1, the ADR adopts a two-stage serial configuration: the first stage utilizes a GGG (Gadolinium Gallium Garnet) salt pill, while the second stage utilizes a CPA (Chromium Potassium Alum) salt pill. Both salt pills are suspended within the bore of the superconducting magnet using 3D-printed PEEK (Polyether Ether Ketone) suspensions for positioning and thermal isolation. The GGG salt pill can provide a cooling temperature below 1K. The temperature sensor leads, heater leads, and PEEK suspension of the CPA salt pill are thermally coupled to the GGG salt pill to reduce heat leakage from 4 K to the CPA salt pill. Two active gas gap heat switches are used to control the heat flow.

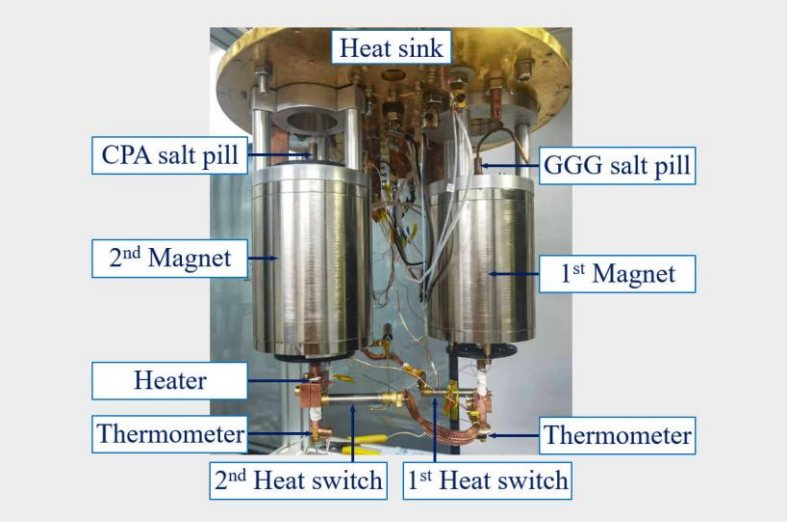

Figure 1. Experimental apparatus.

We did not study the temperature fluctuations of the GGG salt pill, but instead focused on the temperature fluctuations of the CPA salt pill during isothermal demagnetization at 49 mK (Since pure proportional control was implemented in the 50 mK stability tests of the earlier study, which are not shown in this paper, the target temperature had to be set below 50 mK to compensate for steady-state error. Consequently, all tests adopted 49 mK as the target temperature.). Therefore, we will primarily introduce the configuration of the CPA stage. For the CPA stage, temperature measurement is performed using a Lake Shore RX-102B-RS temperature sensor, and temperature data is collected using a Lake Shore Model 372 AC resistance bridge. The superconducting magnet

of 4 T@14.1 A is utilized to generate the required magnetic field. Test results show that the lowest temperature of this two-stage ADR system can reach 26.4 mK, and it can maintain 1.5 h at 50 mK under a 5 μW electrical heating load. The heat leakage to the CPA salt pill during isothermal demagnetization at 50 mK is estimated to be 4.24 μW.

The magnet current controls the magnitude of the magnetic field, and the magnitude of the magnetic field controls the temperature. Therefore, the magnet power supply is crucial to this study. Two different magnet power supplies were used for the testing. The first magnet power supply is the Lake Shore Model 625 superconducting magnet power supply. The second one is the Keithley Model 2602B System SourceMeter. During the isothermal demagnetization at 49 mK, we applied 1 μW of heating power to the CPA salt pill. The stability of the heating power also affects temperature stability. The Tonghui 6402B power supply was used as the power supply for the heater, and the resolution of this power supply is 1 mV.

2.2 Laboratory Noise Analysis

The laboratory is equipped with two chillers for the pulse tube cryocooler compressor, a vacuum pump, and other equipment, where the pulse tube cryocooler compressor is installed in an adjacent room. During the experiment, we clearly observed that the startup or shutdown of the chiller compressor sometimes caused significant interference with temperature measurements of the ADR, while the effects of other equipment on temperature measurements remain unclear. Many attempts were made, including grounding the shielded layer of temperature measurement cables, wrapping the exposed temperature measurement cables joint with aluminum foil, changing the grounding location of the Model 372 or experimental bench, and using different settings for the Model 372.

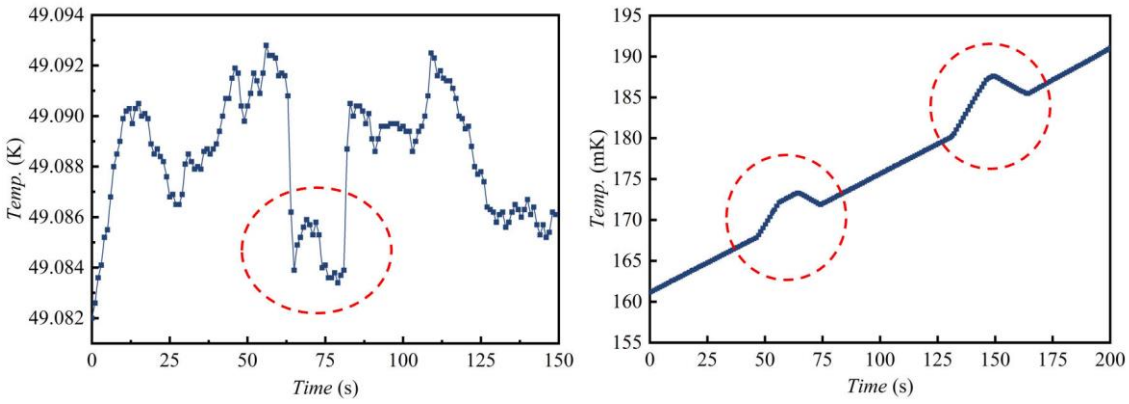

Figure 2. Interference from the chiller on temperature measurement (left); Testing the system shielding effect using a walkie-talkie (right).

These combined measures reduced the frequency and intensity of interference from the chiller, but did not eliminate it completely. Figure 2 shows the temperature measurement interference caused by the startup or shutdown of the chiller compressor during the CPA isothermal demagnetization process. Therefore, subsequent tests were conducted with interference present. A walkie-talkie with 4 W transmission power was used to test the shielding effect of the improved temperature measurement cables, as shown in Figure 2. This is a heating-up process, and the noticeable temperature fluctuations in the figure were caused by two brief

activations of the walkie-talkie. This also indicates that the shielding of the temperature measurement wiring needs further improvement.

3. Temperature control system

The temperature control system is shown in Figure 3, where T_{set} is the target temperature, T_t is the measured temperature, e_t is the error, S_t is the control signal, P_t is the output value, d_t is the external disturbance, and $T_{t,\,ture}$ is the truth temperature. A self-developed LabVIEW program is utilized for reading and recording temperature data from the Model 372, while a PID control algorithm, also written in LabVIEW, is employed for controlling the system. The PID control equation is shown in equation (1), where K_P is the proportional gain, T_I is the integral time, and T_D is the derivative time.

$$S_t = K_P\left(e_t + \frac{1}{T_I}\int e_t \mathrm{d}t + T_D\frac{\mathrm{d}e_t}{\mathrm{d}t}\right) \tag{1}$$

The PID parameters were manually adjusted, and their settings have a significant impact on stability. Different control strategies require different parameters. After multiple adjustments, although the optimal PID parameters were not determined, we preliminarily identified a suitable parameter range. Relevant parameters in subsequent experiments were based on this established range. The PID controller outputs the control signal S_t to the magnet power supply, with the control signal being either a current or voltage signal. Current control was implemented using either the Model 625 or 2602B, while voltage control was implemented using the 2602B. Because of the inductance of the superconducting coil, we supposed that using current mode might be better than voltage mode. Furthermore, the extremely low resistance of the superconducting coil loop, which was unfavorable for voltage control, a 1 Ω bias resistor was incorporated into the circuit when using the Model 2602B as the magnet power supply. The superconducting magnet power supply outputs the corresponding value based on the control signal, thus achieving temperature control.

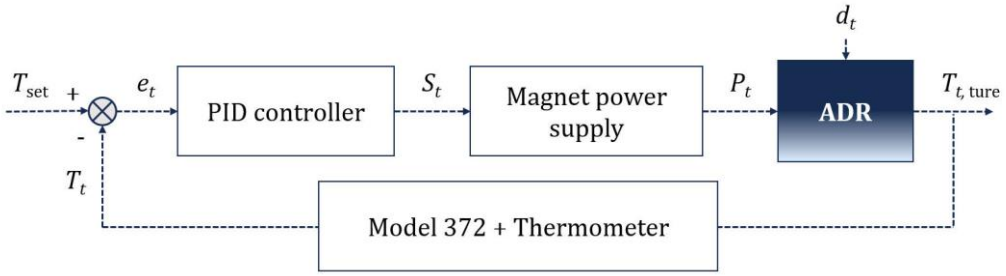

Figure 3. Schematic diagram of the temperature control system.

The excitation current of the temperature sensor from the Model 372 also affects the measurement. A higher excitation current better suppresses the noise but induces stronger self-heating effects, causing the measured temperature T_t to deviate from the true temperature $T_{t,\,ture}$. Based on the manual and post-test considerations, an excitation current of 31.6 nA was selected.

4. Experimental results

The resolution of the magnet power supply affects the resolution of the magnetic field. For the Model 625, the current resolution is 100 μA, which translates to a magnetic field resolution of 28.4 μT for the magnet it controls. The PID controller uses current control. The temperature curve is shown in Figure 4. The RMSE of 49 mK isothermal demagnetization within 2 hours is 11.79 μK.

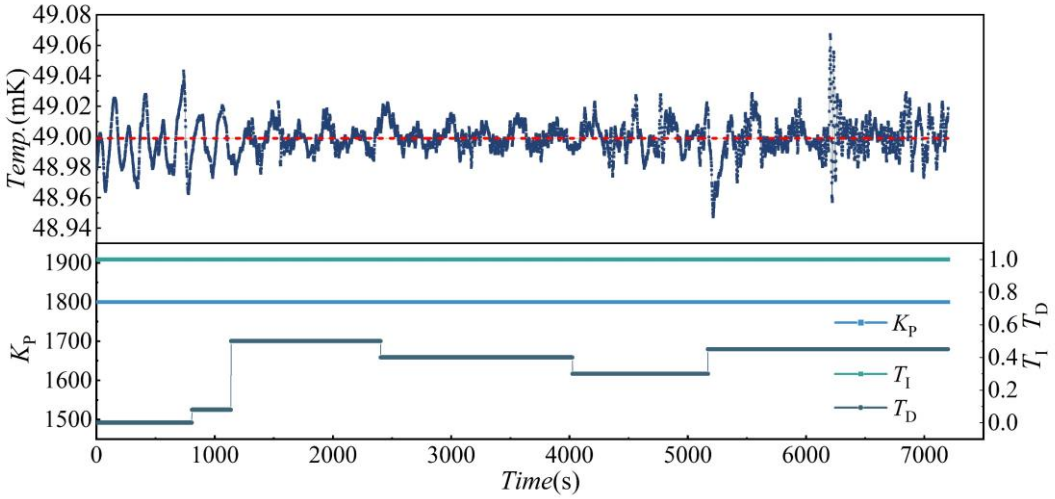

Figure 4. 49mK isothermal demagnetization: Model 625 was used as the power supply for the magnet, with current control (the red line represents the average temperature)

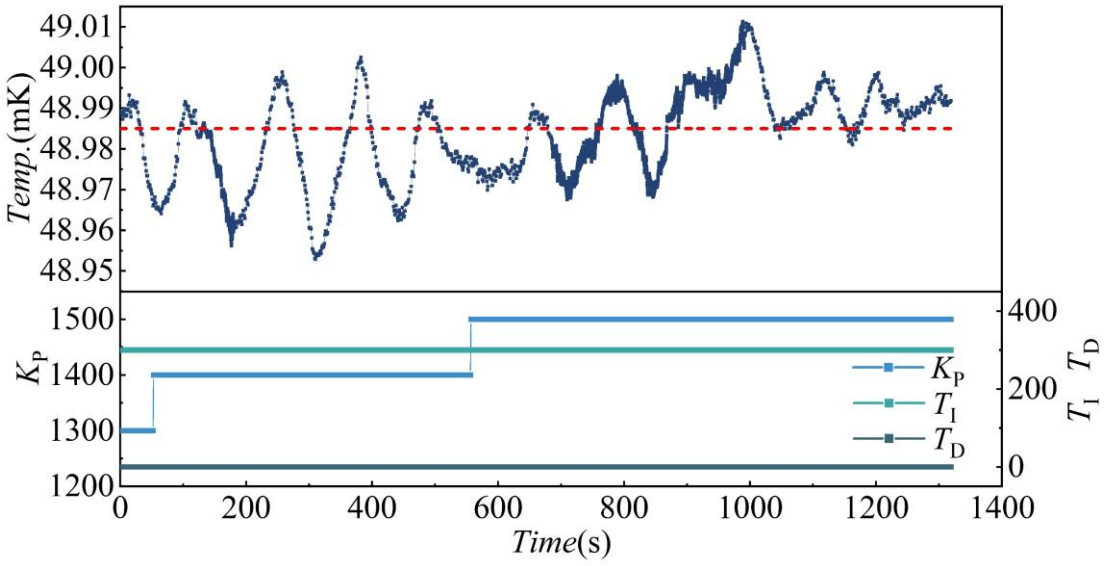

Figure 5. 49mK isothermal demagnetization: Model 2602B was used as the power supply for the magnet, with voltage control (the red line represents the average temperature).

To further enhance the magnetic field resolution, the Model 2602B was employed as the power supply. The resolution of the 2602B in voltage mode is 50 μV. As previously mentioned, a

1 Ω bias resistor was added to the magnet circuit, and the total impedance of the circuit fluctuates around an average value of 1.19 Ω. Therefore, the current resolution in the circuit is approximately 42 μA, corresponding to 11.9 μT magnetic field resolution in the controlled magnet. The temperature curve is shown in Figure 5. In this control mode, the RMSE within 22 minutes is 11.02 μK. During the test, different sampling frequencies were used with the Model 372, and no significant impact on the results was observed.

Subsequently, the 2602B was switched to current mode with a 20 μA resolution. This means the resolution of the magnet it controls is 5.67 μT. The temperature curve is shown in Figure 6. Under this setup, the RMSE of the ADR over 1.6 hours is 4.12 μK. The setting of the 372 filter time affects the temperature measurement results. In this control mode, we investigated the impact of different filter times on temperature control, as shown in Figure 6. The filter time influences the peak and period of the fluctuation and is related to the PID parameter settings. Among the tested filter times, the best temperature stability was achieved with an 18s filter time.

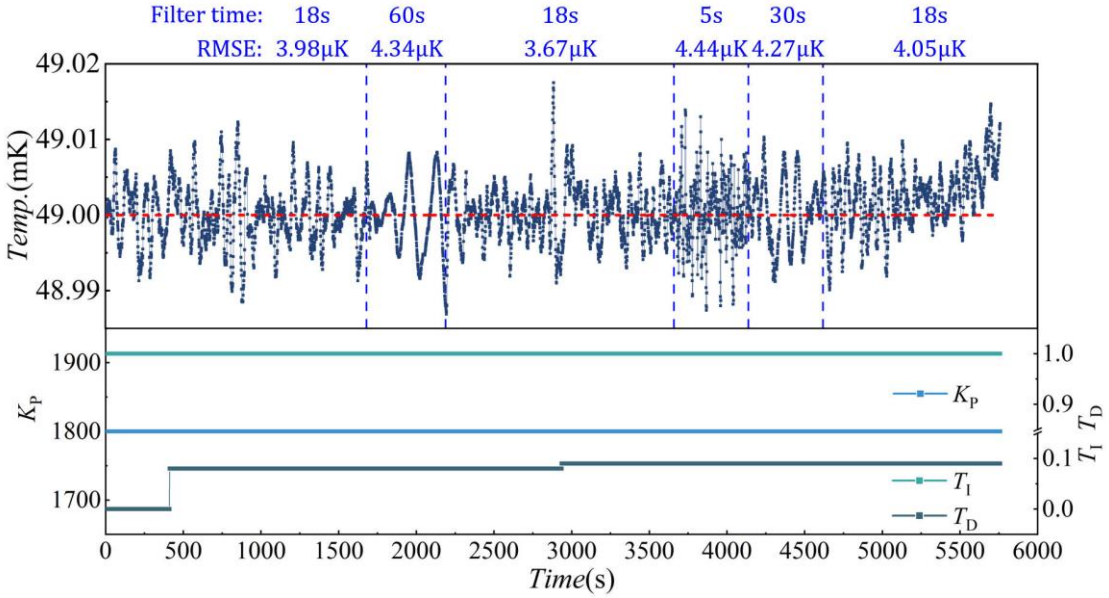

Figure 6. 49mK isothermal demagnetization: Model 2602B was used as the power supply for the magnet, with current control (the red line represents the average temperature).

The test was conducted under the interference of the chiller, which is one of the main factors limiting further improvement in temperature stability. The compressor of the chiller was manually turned off for approximately 10 minutes at around 1.4 hours into the experiment. During this period, the chiller's circulating water pump remained operational, utilizing the thermal capacity of the stored water to maintain pulse tube cryocooler operation. Within this timeframe, an RMSE of 1.99 μK was achieved during a 262 second interval, representing a significant improvement compared to the RMSE of 4.12 μK.

5. Conclusion

To improve the temperature stability of refrigerators in the sub-Kelvin temperature range and enhance the ability to support future applications, temperature control studies on ADR were

conducted. An analysis of the electromagnetic noise sources affecting ADR stability was performed. Since noise source could not be removed, methods were adopted to strengthen the noise shielding capability, although complete elimination of interference was not achieved. In the presence of chiller compressor interference, different control strategies and magnet power supplies were tested, achieving stability of 4.12 μK RMSE over a period of 1.6 hours at 49 mK. During the brief shutdown of the chiller compressor, the temperature fluctuation dropped to 1.99 μK within a 262 second period. This reveals insufficient shielding of the measurement circuit while indicating the system's potential for further improvement. Future work will be done to further optimize the performance.

Acknowledgments

This work was supported by the National Key Research and Development Program of China (Grant No 2022YFB3505100), the Strategic Priority Research Program of the Chinese Academy of Sciences (Grant No XDB1270300), and the National Science Fund for Distinguished Young Scholars (Grant No 51925605).

References

[1] Shirron P, Canavan E, DiPirro M, et al. Development of a cryogen-free continuous ADR for the constellation-X mission[J]. Cryogenics, 2004, 44(6-8): 581-588.
[2] Shinozaki K, Mitsuda K, Yamasaki N Y, et al. Development of double-stage ADR for future space missions[J]. Cryogenics, 2010, 50(9): 597-602.
[3] Wang Chang, Li Ke, Shen Jun, et al. Ultra-low temperature adiabatic demagnetization refrigerator for sub-Kelvin region[J]. Acta Phys. Sin., 2021, 70(9): 263-269.
[4] Ding J, Jin H, Shen J. A μK-level temperature stability control method for TES energy resolution test[J]. Journal of Low Temperature Physics, 2022, 209(5-6): 1212-1217.
[5] Woo K R, Kim H B, Kim H L, et al. An MMC-based temperature control system for a long-term data collection[J]. Journal of Low Temperature Physics, 2022, 209(5): 1218-1225.
[6] Shirron P J. Applications of the magnetocaloric effect in single-stage, multi-stage and continuous adiabatic demagnetization refrigerators[J]. Cryogenics, 2014, 62: 130-139.
[7] Pobell F. Matter and methods at low temperatures[M]. 3rd, rev.expanded ed ed. Berlin ; New York: Springer, 2007.
[8] Jahromi A E, Shirron P J. Compact and efficient continuous adiabatic demagnetization refrigerator for line emission mapper[J]. Journal of Astronomical Telescopes, Instruments, and Systems, 2023, 9(4): 041003.
[9] Shirron P, Wegel D, DiPirro M, et al. An adiabatic demagnetization refrigerator capable of continuous cooling at 10mK and below[J]. Nuclear Instruments and Methods in Physics Research Section A: Accelerators, Spectrometers, Detectors and Associated Equipment, 2006, 559(2): 651-653.
[10] Shirron P J, Kimball M O, DiPirro M J, et al. Performance Testing of the Astro-H Flight Model 3-stage ADR[J]. Physics Procedia, 2015, 67: 250-257.
[11] Shirron P J, Kimball M O, James B L, et al. Operating modes and cooling capabilities of the 3-stage ADR developed for the Soft-X-ray Spectrometer instrument on Astro-H[J]. Cryogenics, 2016, 74: 2-9.